Available online at www.sciencedirect.com
ScienceDirect
Materials Chemistry and Physics 108 (2008) 82–87
MATERIALS CHEMISTRY AND PHYSICS
www.elsevier.com/locate/matchemphys

The changes of morphology, structure and optical properties from carbon nanotubes treated by hydrogen plasma

Leyong Zeng [a,b], Weibiao Wang [a,*], Jingqiu Liang [c], Zhiqian Wang [d], Yuxue Xia [a,b], Da Lei [a,b], Xinguang Ren [a], Ning Yao [d], Binglin Zhang [d]

[a] *Key Laboratory of Excited State Processes, Changchun Institute of Optics, Fine Mechanics and Physics, Chinese Academy of Sciences, Changchun 130033, PR China*
[b] *Graduate School of Chinese Academy of Sciences, Beijing 100049, PR China*
[c] *State Key Laboratory of Applied Optics, Changchun Institute of Optics, Fine Mechanics and Physics, Chinese Academy of Sciences, Changchun 130033, PR China*
[d] *Key Laboratory of Materials Physics of Education Ministry of China, Department of Physics, Zhengzhou University, Zhengzhou 450052, PR China*

Received 14 May 2007; received in revised form 1 September 2007; accepted 6 September 2007

Abstract

In this paper, carbon nanotubes synthesized by floating catalyst method were purified by liquid-phase oxidation method and treated by hydrogen plasma with different time. The morphology and microstructure of carbon nanotubes were characterized by transmission electron microscope (TEM), high-resolution transmission electron microscope (HRTEM), selected area electron diffraction (SAED) and Raman spectroscope. The results showed that carbon nanotubes with bamboo-like structure changed solid and helical structure with the treatment of hydrogen plasma for 5 h and 10 h, and the intensity of D peak in Raman spectrum was larger and larger. The UV–vis absorption spectrum indicated that the absorption peak of treated carbon nanotubes was redshifted, stronger and narrower than that of untreated carbon nanotubes. However, the effect of hydrogen plasma treatment on the FT-IR spectrum of carbon nanotubes was slight. The results probably made carbon nanotubes have important applications in optical absorption material with controllable wavelength.

Keywords: Carbon nanotubes; Hydrogen plasma; Microscope; Optical properties

1. Introduction

Since their discovery by Iijima in 1991 [1], carbon nanotubes (CNTs) have attracted considerable attention because of their unique structure, electric, optical and mechanical properties [2–4]. Much effort has been made in the study of their potential applications, especially in optics and field emission [5–7]. However, the CNTs synthesized by chemical vapor deposition (CVD) method (including floating catalyst method) are disadvantaged for the applications in optical and electronic devices because of the presence of impurities, which can lead to the unstable performances of CNTs. Some methods have been used to improve the properties of CNTs [8–11]. The technology of hydrogen plasma treatment is a simple and effective method, which can change the morphology and structure of CNTs and simultaneously avoid the introduction of other noncarbonous impurities. Recently, some authors reported that CNTs can be transformed into nanodiamonds by hydrogen plasma treatment [12–14]. Also, the field emission property of CNTs can be improved by hydrogen plasma treatment because of the bend of graphitic sheets [15–17]. However, the obtained results are different in different conditions of hydrogen plasma treatment, which could lead to the different properties of treated CNTs.

In this paper, we tried to investigate the changes of morphology, microstructure and optical properties of CNTs by hydrogen plasma treatment with different time. The morphology and microstructure of CNTs were characterized by TEM, HRTEM and Raman spectrum. Finally, the UV–vis absorption spectrum and FT-IR spectrum of untreated and treated CNTs with hydrogen plasma for 5 h and 10 h were also analyzed.

* Corresponding author. Tel.: +86 431 86176339; fax: +86 431 86176339.
E-mail address: wangwbt@126.com (W. Wang).

0254-0584/$ – see front matter © 2007 Elsevier B.V. All rights reserved.
doi:10.1016/j.matchemphys.2007.09.004

Table 1
The experimental parameters of hydrogen plasma treatment

Samples	Microwave power (W)	Reaction temperature (K)	Reaction pressure (kPa)	H_2 flow rate (sccm)	Reaction time (h)
a	–	–	–	–	–
b	1600	1073	6	100	5
c	1600	1073	6	100	10

2. Experimental

The CNTs were synthesized by floating catalyst method at the temperature of 1023 K, using C_2H_2 as carbon source, N_2 as carrier gas and ferrocene as catalyst precursor. The purification of CNTs were made by liquid-phase oxidation method. First CNTs were immersed in the solution of hydrofluoric acid with the concentration of 25% for 10 h. Then CNTs were boiled and immersed in the solution of H_2SO_4/HNO_3 with the ratio of 3/1 for 60 min and 12 h, respectively. Finally, they were dried at the temperature of 473 K. The CNTs must be rinsed with deionised water in every step.

The hydrogen plasma treatment of CNTs was carried out by microwave plasma-enhanced CVD (MPECVD) method. The schematic diagram of MPECVD setup was shown in Fig. 1. Before the experiment, the powder of purified CNTs was dispersed onto a salver of Al_2O_3. The temperature of substrate was controlled by microwave power and chamber pressure. The microwave power increased gradually from 800 W. After it increased to 1600 W and the system was stable, the gas of H_2 was introduced. The experimental parameters were shown in Table 1. For the samples of untreated and treated by hydrogen plasma for 5 h and 10 h, respectively, the morphology and microstructure were characterized by Tecnai F 30 TEM and HRTEM (with the accessory of SAED) and Jobin Yvon HR800 Raman spectroscope. The UV–vis absorption spectrum and FT-IR spectrum were tested by UV-3101PC scanning spectrophotometer and Bio-Red FTS-3000 (Excalibur series), respectively.

3. Results and discussion

Fig. 2(a) and (b) shows the images of CNTs untreated by hydrogen plasma. It can be observed from Fig. 2(a) that CNT has distinctly bamboo-like structure. The outer wall of CNT is smooth and comparatively straight. In the inset of Fig. 2(a), the SAED pattern of CNTs indicates the presence of the crystal-plane (0 0 2), (1 0 0) and (1 1 0). The intensity of (0 0 2) is largest in all. In Fig. 2(b), the graphitic sandwich of CNT can be seen clearly, which indicates the completed structure of CNT. The inset of Fig. 2(b) further shows the parallel graphite layers, and the space between every two layers is about 0.338 nm.

The images of CNTs treated by hydrogen plasma for 5 h are shown in Fig. 2(c) and (d). In comparison with the CNTs untreated by hydrogen plasma, it can be found that the wall of CNT is slightly curving. The inner diameter is small, even

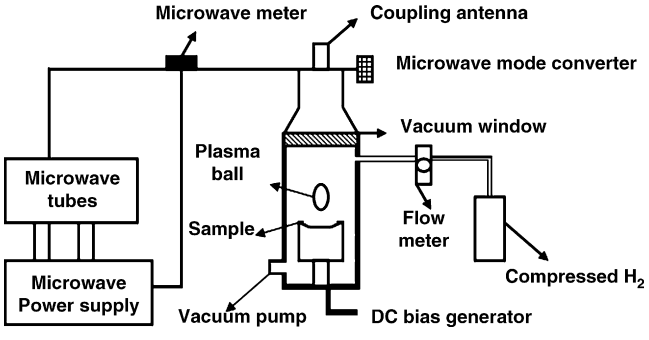

Fig. 1. The schematic diagram of MPECVD experimental setup.

disappears in some regions (arrows in Fig. 2(c)). In the inset of Fig. 2(c), the SAED pattern is similar to that of untreated CNTs except the weak intensity of (0 0 2). Fig. 2(d) shows that the inner layers of CNT has disordered structure, but the outer graphite layers are still parallel to the axis direction of CNT. The inset of Fig. 2(d) indicates that the completed graphite layers of CNT have been destroyed. Probably, the change of CNTs core was brought by the destroyed graphite layers. In the process of hydrogen plasma treatment, some C–C bonds were cut at the defects of CNTs and others were replaced by C–H bonds, which led to the discontinuity of carbon rings. The incomplete graphitic layers may sink into the CNTs core at the discontinuity of carbon rings.

Fig. 2(e)–(g) shows the images of CNTs treated by hydrogen plasma for 10 h. It can be found that in Fig. 2(e), the inner diameter of CNTs has completely disappeared. These CNTs are enlaced one another, and they become more curved than CNTs treated by hydrogen plasma for 5 h. Fig. 2(f) shows that the wall of CNT is contorted and has helical structure as a whole. In the inset of Fig. 2(f), the SAED pattern indicates the sharp and bright diffraction rings of CNTs. Differently from the SAED patterns of CNTs untreated and treated for 5 h, the crystal-plane of (1 0 2) is also observed. In Fig. 2(g), the HRTEM image shows that the outer diameter of solid CNT becomes smaller than that of CNT untreated and treated for 5 h because of the helical structure. The inset of Fig. 2(g) indicates the disordered structure of destroyed graphite layers. In comparison with the inset of Fig. 2(d), the discontinuous parallel graphitic layers have entirely turned into out-of-order structure, which is also in accordance with the contorted and helical structure of CNTs in Fig. 2(d).

Raman spectrum is a powerful tool of characterizing the microstructure of CNTs. Fig. 3 shows the Raman spectrum of untreated and treated CNTs. It indicates the presence of two strong peaks at about 1351 cm^{-1} and 1572 cm^{-1}, commonly known as the first-order D and G bands of CNTs. The peak at about 1571 cm^{-1} corresponds to an E_{2g} mode of graphite, which is due to the sp^2-bonded carbon atoms in a two-dimensional hexagonal graphitic layer. The D band at about 1351 cm^{-1} is associated with the presence of defects in the hexagonal graphitic layers [18,19]. Furthermore, the two-order D peak at about 2708 cm^{-1} is also observed. It can be found from Fig. 3 that all the Raman peaks have tiny blueshift after CNTs were treated by hydrogen plasma, and the blueshift is larger with the longer treatment time of hydrogen plasma. The ratio of the intensity of the D and G bands is known to be correlated to the quality of CNTs, which is used to estimate the degree of disorder in graphitic carbon [18]. By calculation, the I_D/I_G ratios of samples (a), (b) and (c) are found to be 0.578, 0.873 and 1.110,

respectively. The strong D peak of treated CNTs was attributed to the wave structure of carbon sheets in tubes. It was estimated that the in-plain graphite crystallite size of untreated CNTs was $L = 4.4\,\text{nm} \times (I_D/I_G)^{-1} = 7.61\,\text{nm}$. For the CNTs treated for 5 h and 10 h, respectively, $L = 5.04$ and 3.96 nm, respectively [20]. These results indicate that the structure of graphitic layers has been destroyed by the treatment of hydrogen plasma. The treatment time of hydrogen plasma is longer, the degree of disorder of graphitic carbon is larger, which is also in accordance with the analysis of HRTEM.

The UV–vis absorption spectrum of untreated and treated CNTs is shown in Fig. 4. Before the test of UV–vis absorption spectrum, CNTs are dispersed in the solution of ethanol, and the ratio of CNTs versus ethanol is 2 mg versus 100 ml. Curve (a) is the UV–vis absorption spectrum of untreated CNTs. A very broad absorption peak appears at about 254 nm, which originates from the C=C structure of CNTs. After CNTs were treated by hydrogen plasma for 5 h, the position of absorption peak has slight redshift and the intensity of absorption is stronger than that of untreated CNTs, which can be observed in curve (b). However, in curve (c), the absorption intensity of CNTs treated for 10 h becomes weaker than that of CNTs treated for 5 h. The absorption peak has distinct redshift and is narrower than that of curves (a) and (b). On the one hand,

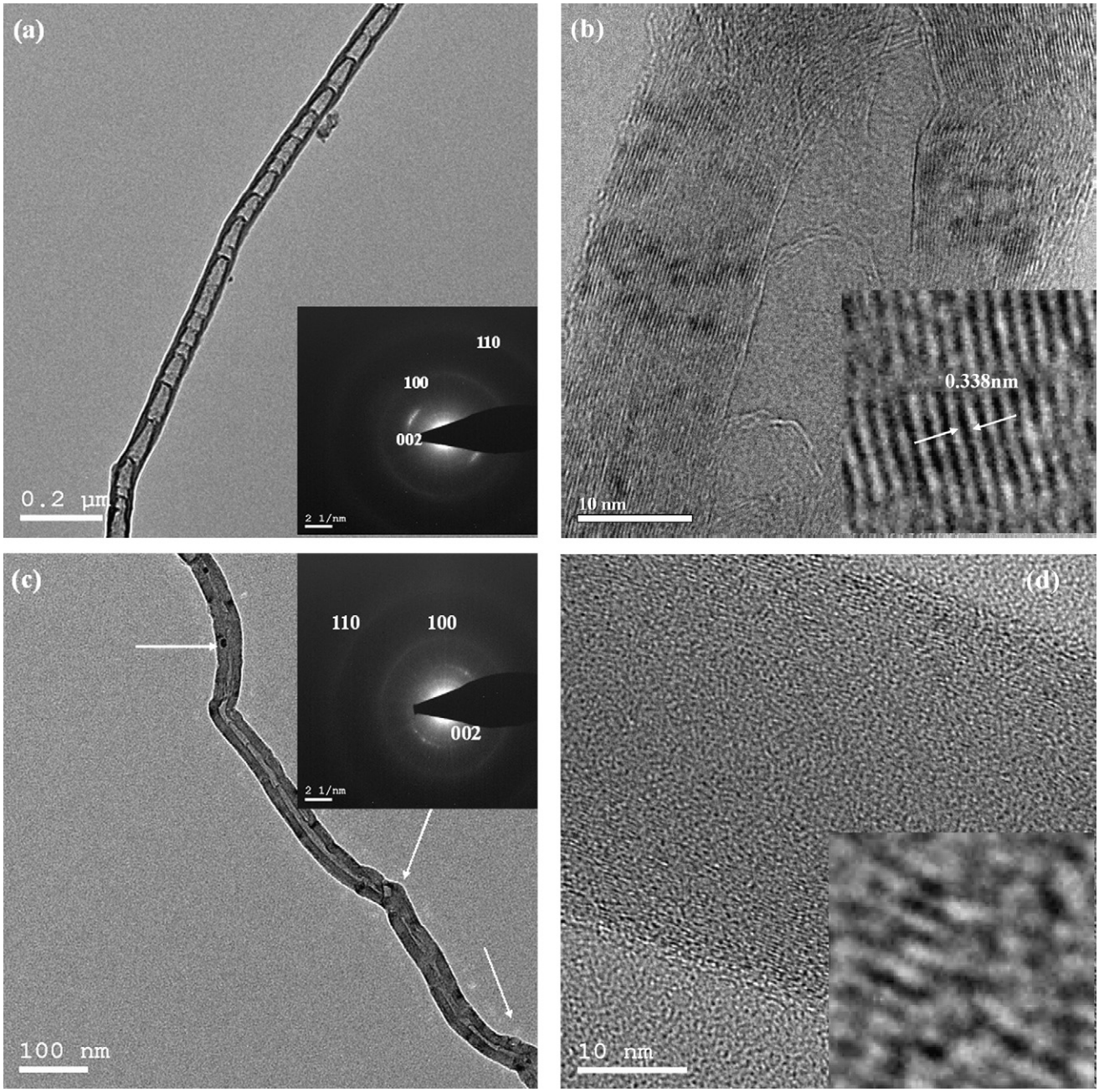

Fig. 2. TEM, HRTEM and SAED images of CNTs untreated and treated by hydrogen plasma: (a, b) untreated; (c, d) treated for 5 h; (e–g) treated for 10 h by hydrogen plasma.

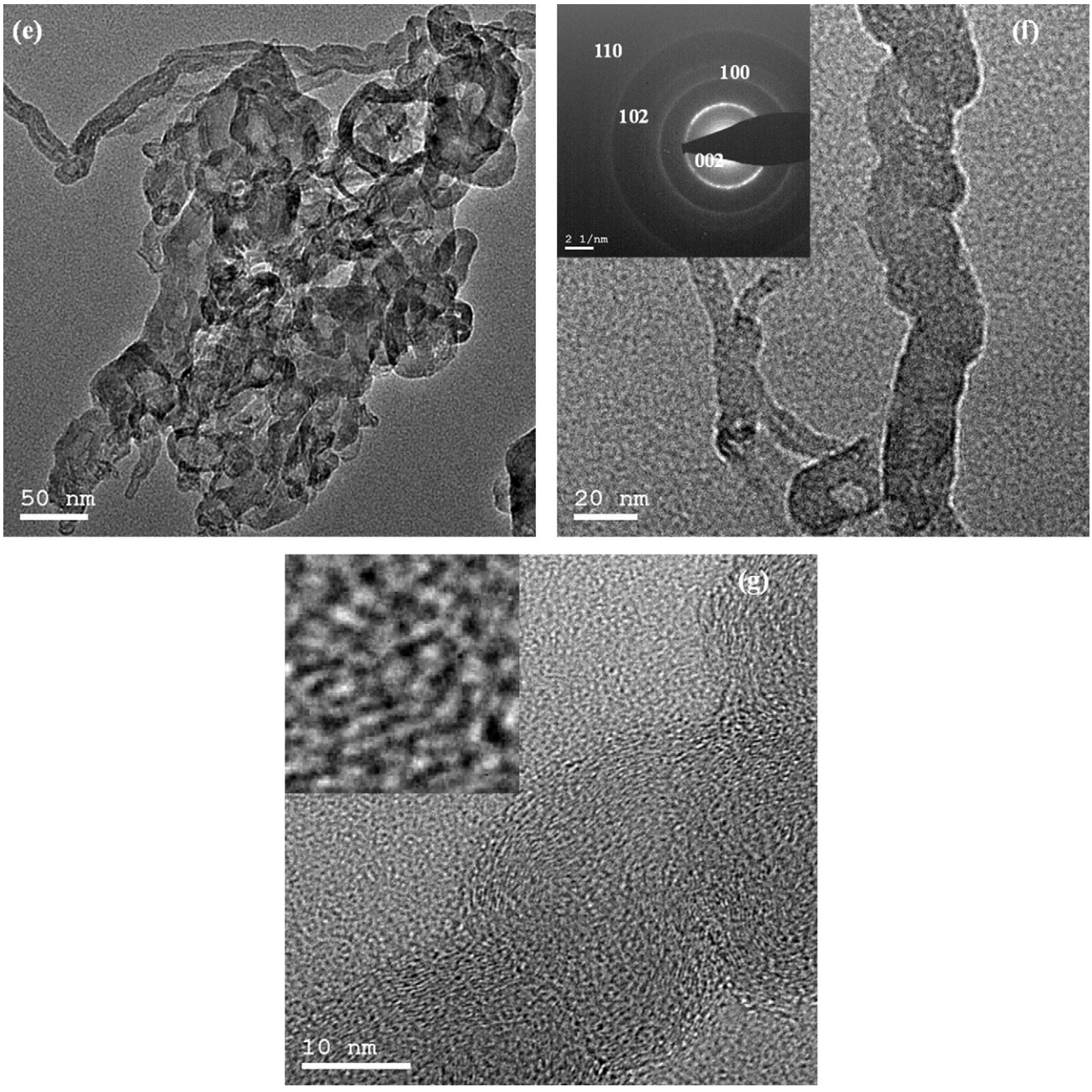

Fig. 2. (*Continued*).

the treatment of hydrogen plasma destroyed the layered structure of carbon nanotubes, which changed the layer interaction and light scattering property of carbon nanotubes. On the other hand, the width and position of absorption peak were also related to the ratio of inner radius (r) versus outer radius (R) of carbon nanotubes. Thinner carbon nanotubes with large value of r/R tended to have their peaks position redshifted and to have narrower peaks [21]. By hydrogen plasma treatment, the inner walls of carbon nanotubes were destroyed and only outer walls had completed layered structure, which were shown in HRTEM images of carbon nanotubes. The thinner completed graphitic layers led to the redshift and narrowness of absorption peak. Furthermore, the absorption peak of carbon nanotubes could be attributed to the π-plasmon resonance in dielectric tensor of carbon nanotubes. The π-plasmon represented a plasma oscillation of delocalized states polarized along the nanotubes axis and the collective excitation of the π-electron system, in which the dispersion relation of π-plasmon was similar to that of the graphite plane [22,23]. The redshift of absorption peak was predicted to arise from an enhanced coupling of the π-plasmon density fluctuations on the inner and outer surfaces of carbon nanotubes [24]. The destroyed and curved inner graphitic layers which was introduced by hydrogen plasma treatment changed the interaction between outer and inner layers, and the discontinuous inner graphitic structure could also change the interaction between π-electron system, which

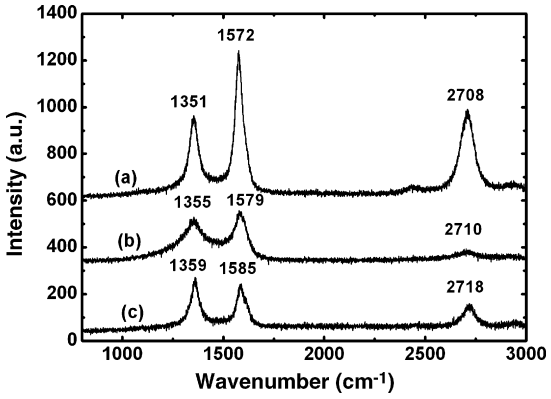

Fig. 3. Raman spectrum of CNTs untreated and treated by hydrogen plasma: (a) untreated; (b) treated for 5 h; (c) treated for 10 h by hydrogen plasma.

brought the redshift and narrowness of absorption peak of carbon nanotubes.

Fig. 5 shows the FT-IR spectrum of different samples. The carbonyl stretch and the C–O bond stretch are observed at about 1703 cm^{-1} and 1155 cm^{-1}, respectively. The peak at about 1703 cm^{-1} originated from the carbonyl stretch of the carboxylic acid groups of the purification treatment and the peak at about 1155 cm^{-1} may be attributed to the C–O bond stretches of CNT–O–C and C–OH units. The peaks at about 1299 cm^{-1} and 1580 cm^{-1} were assigned for bending of C–H (out-of-plain) and bending of C–H (in-plain). The peaks at about 962 cm^{-1} and 1400 cm^{-1} were related to –OH vibration and stretch. The peak at about 1089 cm^{-1} was the overlap of C–O stretch and C–C stretch. Comparing the three curves in Fig. 5, the weak peak at about 1580 cm^{-1} appeared after CNTs were treated by hydrogen plasma, which was brought by C–H bond. These results indicate that the treatment of hydrogen plasma does not introduce new functional groups other than C–H bond.

In our experiment, the treatment of hydrogen plasma changed the morphology and destroyed the graphitic layers structure of CNTs, but the graphitic structure of CNTs was not changed. The CNTs with high-quality has ordered sandwich of graphite and small defects. After CNTs were treated by hydrogen plasma, the disordered structure of graphite and the defects of graphite were formed. With the increase of treatment time, the defects and disordered degree were stronger and stronger, moreover, the inner walls of CNTs were changed prior to the outer walls. On the one hand, it was arosen from the hydrogen plasma; on the other hand, it came from the high temperature treatment of 1073 K for 5 h and 10 h, respectively. First, the inner shell rearrangement of CNTs happened by the high temperature. In the process of inner shell rearrangement, the inner shell was destroyed and broken and the C–C bonds were partly replaced by C–H bonds with the effect of hydrogen plasma. About the reaction between hydrogen and inner carbon atoms, on the one hand, the surface defect sites of CNTs played a role as a hydrogen approaching path; on the other hand, the tops of CNTs were opened partly by the purification of CNTs, which also increased the reaction between hydrogen plasma and inner layers of CNTs. Hydrogen plasma treatment changed the morphology and structure of CNTs, and it is also significative for the further investigation of optical properties and optical applications of CNTs, especially as light-invisible material with controllable wavelength.

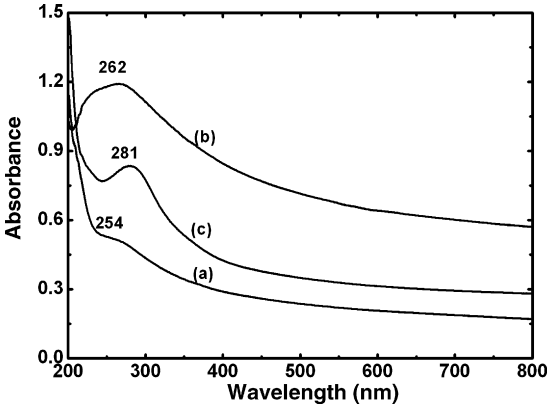

Fig. 4. UV–vis absorption spectrum of CNTs untreated and treated by hydrogen plasma: (a) untreated; (b) treated for 5 h; (c) treated for 10 h by hydrogen plasma.

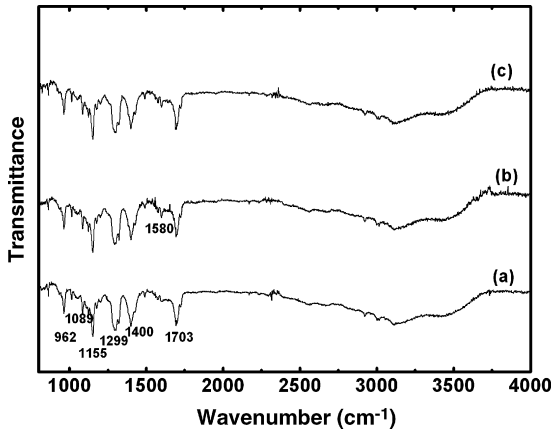

Fig. 5. FT-IR spectrum of CNTs untreated and treated by hydrogen plasma: (a) untreated; (b) treated for 5 h; (c) treated for 10 h by hydrogen plasma.

4. Conclusions

In this paper, purified CNTs with bamboo-like structure turned into solid and helical structure by the treatment of hydrogen plasma for 5 h and 10 h, respectively, and the parallel and complete graphitic layers have become defective and disordered. However, the treatment of hydrogen plasma did not change the graphitic structure of CNTs. The UV–vis absorption band of CNTs had slight redshift and the absorption peak was narrower than that of untreated CNTs with the increase of treatment time. However, the treatment of hydrogen plasma had only slight effect on the FT-IR spectrum of CNTs.

Acknowledgements

This research work was supported by the National Natural Science Foundation of China (NSFC, Grant Nos. 50072029 and 50572101). The authors would also like to thank Prof. Liping You and Guorui Wang for TEM, HRTEM and Raman spectrum analysis.

References

[1] S. Iijima, Nature 354 (1991) 56.
[2] R.H. Baughman, A.A. Zakhidov, W.A. de Heer, Science 297 (2002) 787.
[3] C.N.R. Rao, B.C. Satishkumar, A. Govindaraj, M. Nath, Chem. Phys. Chem. 2 (2001) 78.
[4] S. Subramoney, Adv. Mater. 10 (1998) 1157.
[5] W.A. de Heer, A. Chatelain, D. Ugarte, Science 270 (1995) 1179.
[6] W.B. Choi, D.S. Chung, J.H. Kang, H.Y. Kim, Y.W. Jin, I.T. Han, et al., Appl. Phys. Lett. 75 (1999) 3129.
[7] L. Vivien, E. Anglaret, D. Riehl, F. Hache, F. Bacou, M. Andrieux, F. Lafonta, C. Journet, C. Goze, M. Brunet, P. Bernier, Opt. Commun. 174 (2000) 271.
[8] Z.X. Jin, X. Sun, G.Q. Xu, S.H. Goh, W. Ji, Chem. Phys. Lett. 318 (2000) 505.
[9] C.S. Chen, X.H. Chen, B. Yi, T.G. Liu, W.H. Li, L.S. Xu, Z. Yang, H. Zhang, Y.G. Wang, Acta Mater. 54 (2006) 5401.
[10] H.J. Kim, I.T. Han, Y.J. Park, J.M. Kim, J.B. Park, B.K. Kim, N.S. Lee, Chem. Phys. Lett. 396 (2004) 6.
[11] S.R.C. Vivekchand, A. Govindaraj, M.M. Seikh, C.N.R. Rao, J. Phys. Chem. B108 (2004) 6935.
[12] L.T. Sun, J.L. Gong, Z.Y. Zhu, D.Z. Zhu, S.X. He, Z.X. Wang, Appl. Phys. Lett. 84 (2004) 2901.
[13] L.T. Sun, J.L. Gong, Z.Y. Zhu, D.Z. Zhu, Z.X. Zhang, W. Zhang, J.G. Hu, Q.T. Li, Diam. Relat. Mater. 14 (2005) 749.
[14] L.T. Sun, J.L. Gong, D.Z. Zhu, Z.Y. Zhu, S.X. He, Adv. Mater. 16 (2004) 1849.
[15] C.Y. Zhi, X.D. Bai, E.G. Wang, Appl. Phys. Lett. 81 (2002) 1690.
[16] K. Yu, Z.Q. Zhu, M. Xu, Q. Li, W. Lu, Chem. Phys. Lett. 373 (2003) 109.
[17] Y.M. Wong, W.P. Kang, J.L. Davidson, B.K. Choi, J.H. Huang, Diam. Relat. Mater. 15 (2006) 1132.
[18] D. Reznik, C.H. Olk, D.A. Neumann, J.R.D. Copley, Phys. Rev. B 52 (1995) 116.
[19] S. Shanmugam, A. Gedanken, J. Phys. Chem. B 110 (2006) 2037.
[20] K. Yu, Z.Q. Zhu, Y.S. Zhang, Q. Li, W.M. Wang, Z.W. Li, T. Peng, Appl. Surf. Sci. 225 (2004) 380.
[21] L. Henrard, A.A. Lucas, P. Lambin, Astrophys. J. 406 (1993) 92.
[22] T. Pichler, M. Knupfer, M.S. Golden, J. Fink, A. Rinzler, R.E. Smalley, Phys. Rev. Lett. 80 (1998) 4729.
[23] R. Friedlein, T. Pichler, M. Knupfer, M.S. Golden, K. Mukhopadhyay, T. Sugai, H. Shinohara, J. Fink, AIP Conf. Proc. 486 (1999) 351.
[24] A.A. Lucas, L. Henrard, P. Lambin, Phys. Rev. B 49 (1994) 2888.